arXiv:1004.0183v1 [cond-mat.stat-mech] 31 Mar 2010

Iterative Schwarz-Christoffel Transformations Driven by Random Walks and Fractal Curves

Fumihito Sato and Makoto Katori*

Department of Physics, Faculty of Science and Engineering,

Chuo University, Kasuga, Bunkyo-ku, Tokyo 112-8551, Japan

(Dated: 31 March 2010)

Abstract

Stochastic Loewner evolution (SLE) is a differential equation driven by a one-dimensional Brownian motion (BM), whose solution gives a stochastic process of conformal transformation on the upper half complex-plane $\mathbb{H}$. As an evolutionary boundary of image of the transformation, a random curve (the SLE curve) is generated, which is starting from the origin and running in $\mathbb{H}$ toward the infinity as time is going. The SLE curves provides a variety of statistical ensembles of important fractal curves, if we change the diffusion constant of the driving BM. In the present paper, we consider the Schwarz-Christoffel transformation (SCT), which is a conformal map from $\mathbb{H}$ to the region $\mathbb{H}$ with a slit starting from the origin. We prepare a binomial system of SCTs, one of which generates a slit in $\mathbb{H}$ with an angle $\alpha\pi$ from the positive direction of the real axis, and the other of which with an angle $(1-\alpha)\pi$. One parameter $\kappa > 0$ is introduced to control the value of α and the length of slit. Driven by a one-dimensional random walk, which is a binomial stochastic process, a random iteration of SCTs is performed. By interpolating tips of slits by straight lines, we have a random path in $\mathbb{H}$, which we call an Iterative SCT (ISCT) path. It is well-known that, as the number of steps N of random walk goes infinity, each path of random walk divided by $\sqrt{N}$ converges to a Brownian curve. Then we expect that the ISCT paths divided by $\sqrt{N}$ (the rescaled ISCT paths) converge to the SLE curves in $N \to \infty$. Our numerical study implies that, for sufficiently large N, the rescaled ISCT paths will have the same statistical properties as the SLE curves have, supporting our expectation.

PACS numbers: 05.40.-a, 05.45.Df, 02.30.-f

*katori@phys.chuo-u.ac.jp

I. INTRODUCTION

One of the highest topics of recent progress in statistical physics of critical phenomena and random fractal patterns is introduction of the Stochastic Loewner Evolution (SLE) by Schramm [1–3]. The SLE will provide a unified theory of statistics of random curves in the plane, which covers (continuum limits of) random interfaces characterizing surface critical phenomena in equilibrium (*e.g.* the percolation exploration process, the critical Ising interface), models of random chains in polymer physics (*e.g.* the self-avoiding walks), fractal patterns playing important roles in non-equilibrium statistical mechanics models (*e.g.* the loop-erased random walks and the uniform spanning trees for sandpile models and forest fire models showing self-organized criticality), and so on [4–6]. The theory is based on two branches of mathematics, the complex function theory [7] and the stochastic analysis [2, 3] and is strongly connected with the conformal field theory [8–10].

As well as by wideness of applications and by richness of mathematics, we are attracted by simple setting of the theory ; Consider a complex plane $\mathbb{C}$. (i) First we consider a motion of Brownian particle on the real axis $\mathbb{R}$. We assume that it starts from the origin 0 at time $t = 0$ and the diffusion constant is given by $\kappa > 0$. If we write the position of the diffusion particle on $\mathbb{R}$ at time $t \geq 0$ as U_t, then $\langle U_t \rangle = 0$ and $\langle U_t^2 \rangle = \kappa t$ for $t \geq 0$. Usually we denote the position of a one-dimensional standard Brownian motion (BM) at time t by B_t, for which $\langle B_t \rangle \equiv B_0 = 0$, $\langle B_t^2 \rangle = t, t \geq 0$. The BM has the scaling property such that for any constant $c > 0$, the distribution of the position of BM at time $c^2 t$ is equal to that of the position of BM at time t multiplied by a factor c, that is, the equality $B_{c^2 t} = cB_t$ holds in distribution. Then we can give the above U_t by

$$U_t = \sqrt{\kappa} B_t, \quad t \geq 0. \tag{1}$$

(ii) Then we solve the following partial differential equation for a complex function $f_t(z)$ on the upper half complex-plane $\mathbb{H} = \{z \in \mathbb{C} : \mathrm{Im}\, z > 0\}$,

$$\frac{\partial f_t(z)}{\partial t} = -\frac{\partial f_t(z)}{\partial z} \frac{2}{z - U_t} \tag{2}$$

under the initial condition $f_0(z) = z$. (iii) Note that the boundary of $\mathbb{H}$ consists of the real axis $\mathbb{R}$ and an infinity point. When $z \in \mathbb{H}$ approaches the special point U_t on $\mathbb{R}$, the position of the BM, the RHS of (2) diverges. If we trace the image of this singular point

$$\gamma_t = f_t(U_t), \quad t \geq 0 \tag{3}$$

we will have a curve $\gamma(0,t] \equiv \{\gamma_s : 0 < s \leq t\}$ in $\mathbb{H}$ starting from the origin. For each $s > 0$ the curve $\gamma(0,s]$ and the region enclosed by parts of the curve and the real axis $\mathbb{R}$ should be eliminated from $\mathbb{H}$ in order to continue to solve Eq.(2) for $t > s$.

For any deterministic simple curve $\gamma(0,t]$ in $\mathbb{H}, t \geq 0$, Loewner proved that there exists a real-valued function U_t and a conformal map f_t, which is one-to-one from $\mathbb{H}$ to $\mathbb{H} \setminus \gamma(0,t] \equiv \{z \in \mathbb{H} : z \neq \gamma_s, 0 < s \leq t\}$, the upper half complex-plane with a slit $\gamma(0,t]$, such that f_t and U_t solve Eq.(2) with the condition (3). The equation (2) is called the Loewner equation [7, 11]. Schramm considered an inverse problem: given U_t on $\mathbb{R}$ and derive a curve $\gamma(0,t]$ by solving Eq.(2). Since he gave U_t by a BM as Eq.(1), γ_t given by Eq.(3) performs a stochastic motion and the obtained curve $\gamma(0,t]$ is statistically distributed in $\mathbb{H}$ [1]. Equation (2) driven by a BM with variance κt is called the stochastic Loewner equation or the Schramm-Loewner evolution (SLE) [12], and a random curve $\gamma(0,t], t \geq 0$ is called the SLE curve with parameter κ (the SLE_κ curve).

Although the change of diffusion constant κ causes only quantitative change of the driving function U_t, that is, scale/time change $\sqrt{\kappa}B_t = B_{\kappa t}$ in distribution, it does qualitative change of SLE_κ curves. When $0 < \kappa \leq 4$, the curve is simple (with no self-intersection) with $\gamma(0,\infty) \subset \mathbb{H}$. When $4 < \kappa < 8$, the curve is self-intersecting and $\gamma(0,\infty)$ hits the real axis $\mathbb{R}$ infinitely many times, but it is not dense on $\mathbb{H} : \gamma(0,\infty) \cap \mathbb{H} \neq \mathbb{H}$ with $\lim_{t\to\infty} |\gamma_t| = \infty$. And when $\kappa \geq 8$, it will cover whole of $\mathbb{H}$ in $t \to \infty$ [2, 3]. The fractal dimension (Hausdorff dimension) of the SLE_κ curve is determined as [13, 14]

$$d^\kappa = \begin{cases} 1 + \kappa/8, & 0 < \kappa < 8 \\ 2, & \kappa \geq 8. \end{cases} \tag{4}$$

Moreover, if κ is chosen to be a special value, SLE_κ curves provide the statistical ensembles of continuous limits of random discrete paths studied in statistical mechanics models exhibiting critical phenomena or in fractal models on lattices. For example, the value $\kappa = 6$ is for the critical percolation model [15, 16]. Effective methods for numerical simulations of SLE_κ curves by computers have been reported [17–19].

Today we can learn from mathematics literatures that the Loewner equation (2) for a deterministic function U_t had played important roles in the complex function theory even before Schramm introduced its stochastic version [7]. We shall say, however, that this equation has not been familiar to us, physicists. More familiar differential equation to us in

the complex calculus is the one, whose solution gives a conformal transformation from $\mathbb{H}$ to the interior of a polygon on the complex plane with mapping the real axis $\mathbb{R}$ to a piecewise linear boundary of the polygon, called the Schwarz-Christoffel transformation (SCT) (see, for example, [20]). So here we try to discuss the Loewner equation (2) by using a special case of SCT.

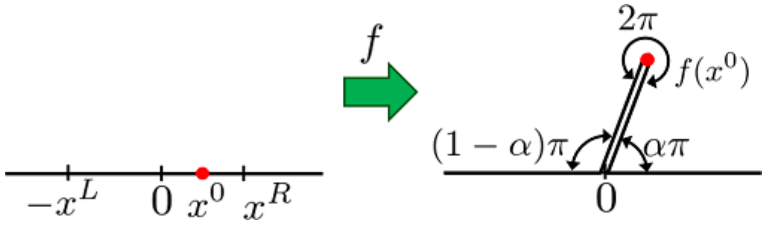


FIG. 1: SCT generating a straight slit in $\mathbb{H}$

Let $0 < \alpha < 1$. Consider a conformal map f from $\mathbb{H}$ to the upper half complex-plane with a straight slit starting from the origin, $\mathbb{H} \setminus \{\text{a slit}\}$, where the angle between the slit and the positive direction of the real axis is $\alpha\pi$ as shown in Fig.1. Since $\mathbb{H}$ with the straight slit can be regarded as a polygon with the interior angles $(1-\alpha)\pi$ on the left side of the origin, 2π around the tip of the slit, and $\alpha\pi$ on the right side of the origin, for any length of a slit, the conformal map is given as an SCT, which solves the differential equation

$$\frac{df(z)}{dz} = b_1(z + x^{\mathrm{L}})^{-\alpha}(z - x^0)(z - x^{\mathrm{R}})^{\alpha-1}, \tag{5}$$

where b_1 is a complex number and $x^{\mathrm{L}}, x^0, x^{\mathrm{R}}$ are real numbers satisfying the inequalities, $x^{\mathrm{L}} > 0, x^{\mathrm{R}} > 0, -x^{\mathrm{L}} < x^0 < x^{\mathrm{R}}$. By this transformation, both of the points $-x^{\mathrm{L}}$ and x^{R} on $\mathbb{R}$ are mapped to the origin, $f(-x^{\mathrm{L}}) = f(x^{\mathrm{R}}) = 0$, and x^0 to the tip of the slit. See Fig.1. We have found the general solution of (5) expressed by

$$\begin{aligned} f(z) &= b_0 + b_1(z + x^{\mathrm{L}})^{1-\alpha}(z - x^{\mathrm{R}})^{\alpha} \\ &\times \left\{1 + \frac{x^0 - x^{\mathrm{R}} + \alpha(x^{\mathrm{L}} + x^{\mathrm{R}})}{x^{\mathrm{L}} + x^{\mathrm{R}}} \frac{\Gamma(1-\alpha)}{\Gamma(2-\alpha)} F\left(1, 1, 2-\alpha; \frac{x^{\mathrm{L}} + z}{x^{\mathrm{L}} + x^{\mathrm{R}}}\right)\right\}, \end{aligned} \tag{6}$$

where b_0 is a complex number, $\Gamma(z) = \int_0^\infty e^{-u}u^{z-1}du$ (the gamma function), and $F(\alpha, \beta, \gamma; z)$ is Gauss's hypergeometric function $F(\alpha, \beta, \gamma; z) = \Gamma(\gamma)/\{\Gamma(\alpha)\Gamma(\beta)\} \sum_{n=0}^\infty \Gamma(\alpha + n)\Gamma(\beta + n)z^n/\{\Gamma(\gamma + n)n!\}$. We impose the hydrodynamic condition

$$\frac{f(z)}{z} \to 1 \quad \text{in} \quad z \to \infty. \tag{7}$$

Then $b_0 = 0, b_1 = 1$ and $x^0 - x^{\mathrm{R}} + \alpha(x^{\mathrm{L}} + x^{\mathrm{R}}) = 0$, and we have $f(z) = (z + x^{\mathrm{L}})^{1-\alpha}(z - x^{\mathrm{R}})^{\alpha}$. Eq.(5) is rewritten in this case as

$$\frac{df(z)}{dz}\frac{2}{z - x^0} = \frac{2f(z)}{(z + x^{\mathrm{L}})(z - x^{\mathrm{R}})}. \tag{8}$$

We then introduce a parameter "time" $t \geq 0$ and assume that x^{L} and x^{R}, and thus also x^0, depend on t by setting

$$f_t(z) = (z + x_t^{\mathrm{L}})^{1-\alpha}(z - x_t^{\mathrm{R}})^{\alpha}. \tag{9}$$

The differential of f_t with respect to t is written as

$$\frac{\partial f_t(z)}{\partial t} = -\frac{2A(z,t)f_t(z)}{(z + x_t^{\mathrm{L}})(z - x_t^{\mathrm{R}})}$$

with $A(z,t) = [-(1-\alpha)(z - x_t^{\mathrm{R}})dx_t^{\mathrm{L}}/dt + \alpha(z + x_t^{\mathrm{L}})dx_t^{\mathrm{R}}/dt]/2$. Let $x_t^{\mathrm{L}} = 2ct^{\beta}, x_t^{\mathrm{R}} = 2t^{\beta}/c$ with constants $c > 0$ and β. Then we can see that, if and only if $c = \sqrt{\alpha/(1-\alpha)}$ and $\beta = 1/2$, $A(z,t)$ becomes independent both of z and t; $A(z,t) \equiv 1$. Combining this observation with Eq.(8) gives the following result: For $0 < \alpha < 1$, the SCT

$$f_t^{\alpha}(z) = \left(z + 2\sqrt{\frac{\alpha}{1-\alpha}}\sqrt{t}\right)^{1-\alpha}\left(z - 2\sqrt{\frac{1-\alpha}{\alpha}}\sqrt{t}\right)^{\alpha} \tag{10}$$

is not only a solution of the Schwarz-Christoffel differential equation (5), but also of the Loewner equation (2) with the driving function

$$\begin{aligned} U_t^{\alpha} &= x_t^0 = x_t^{\mathrm{R}} - \alpha(x_t^{\mathrm{L}} + x_t^{\mathrm{R}}) \\ &= \begin{cases} \sqrt{\kappa^{\alpha} t} & \text{if } \alpha \leq 1/2 \\ -\sqrt{\kappa^{\alpha} t} & \text{if } \alpha > 1/2, \end{cases} \end{aligned} \tag{11}$$

where

$$\kappa^{\alpha} = \frac{4(1-2\alpha)^2}{\alpha(1-\alpha)}. \tag{12}$$

As time t goes, the straight slit performs as an "evolutionary boundary" of the image of $\mathbb{H}$ by f_t, in which the tip of the slit (3) is evolving as

$$\begin{aligned} \gamma_t^{\alpha} &= f_t^{\alpha}(U_t^{\alpha}) \\ &= 2\left(\frac{1-\alpha}{\alpha}\right)^{1/2-\alpha} e^{i\alpha\pi}\sqrt{t}, \quad t \geq 0. \end{aligned} \tag{13}$$

One can observe the equality

$$U_t^{\alpha} = \pm\sqrt{\langle(\sqrt{\kappa^{\alpha}}B_t)^2\rangle}, \quad t \geq 0, \tag{14}$$

since $\langle B_t^2 \rangle = t$. That is, the driving function U_t^α for the above SCT (11) is the positive or the negative root square of the squared average of the random driving function (1) of the SLE. So if we are able to introduce fluctuations into the SCT systematically, we can draw approximations of SLE curves on $\mathbb{H}$. It may be the basic idea to simulate SLE curves by dividing a time period $(0, t]$ into n small intervals $\{(t_{j-1}, t_j] : j = 1, 2, \ldots, n\}$ by setting $0 = t_0 < t_1 < \cdots < t_n = t$ and the above single SCT is replaced by an n-multiplicative map of infinitesimal SCTs with sufficiently large n [17, 18].

On the other hand, we know the fact that the diffusion property of BM can be observed in long-time asymptotic behavior of a simple discrete-time stochastic process, random walk (RW). Let $\sigma_j, j = 1, 2, 3, \ldots$ be independent and identically distributed (i.i.d.) random variables taking values $\sigma_j = 1$ with probability $1/2$ and $\sigma_j = -1$ with probability $1/2$. Consider a simple symmetric RW on the one-dimensional lattice $\mathbb{Z} = \{\ldots, -2, -1, 0, 1, 2, \ldots\}$ starting from the origin 0 at time $n = 0$. We denote the position of the random walker at time $n = 0, 1, 2, \ldots$ by w_n. Then, $w_0 = 0$ and

$$w_n = \sum_{j=1}^{n} \sigma_j, \quad n = 1, 2, 3, \ldots. \tag{15}$$

In the present paper, we consider an SCT as a functional of a random variable σ and consider an Iterative system of SCTs (ISCTs) driven by RW. By this system, each time series of steps $(\sigma_1, \sigma_2, \ldots)$ of RW is mapped to a series of points $(\xi_1, \xi_2, \ldots)$ in $\mathbb{H}$. Let W_n and $\Xi_n, n \geq 0$ be the interpolations by straight lines of w_n and $\xi_n, n = 0, 1, 2, \ldots$, respectively. Since for $T > 0$, $\{W_{Nt}/\sqrt{N} : 0 \leq t \leq T\}$ converges to $\{B_t : 0 \leq t \leq T\}$ as $N \to \infty$ in distribution,

$$\zeta^N(0, T] = \left\{ \frac{\Xi_{Nt}}{\sqrt{N}}, 0 < t \leq T \right\}, \quad T > 0, \tag{16}$$

which we call the rescaled ISCT path with N up to time T, will converge to an SLE curve up to time T, $\gamma(0, T]$, in distribution as $N \to \infty$. Figure 2 shows the rescaled ISCT paths $\zeta^N(0, 1] = \{\Xi_{Nt}/\sqrt{N}, 0 \leq t \leq 1\}$ with $N = 5 \times 10^4$ for $\kappa = 2$ and 6, which are drawn by interpolating the series of points $\{\xi_j/\sqrt{N}\}_{j=0}^N$ by lines. They seems to approximate the SLE_κ curves $\gamma(0, 1]$ very well. In the present paper, we will show that, for sufficiently large N, ζ_t^N has the same statistical properties as the SLE curve γ_t has.

The paper is organized as follows. In Sec.II, we define the ISCT driven by random walk with a parameter $\kappa = \kappa^\alpha$ defined by (12) and the ISCT_κ paths. In Sec.III, by observing the behavior of ISCT paths $\Xi(0, n]$ for small values of n, we show that, even if we use the

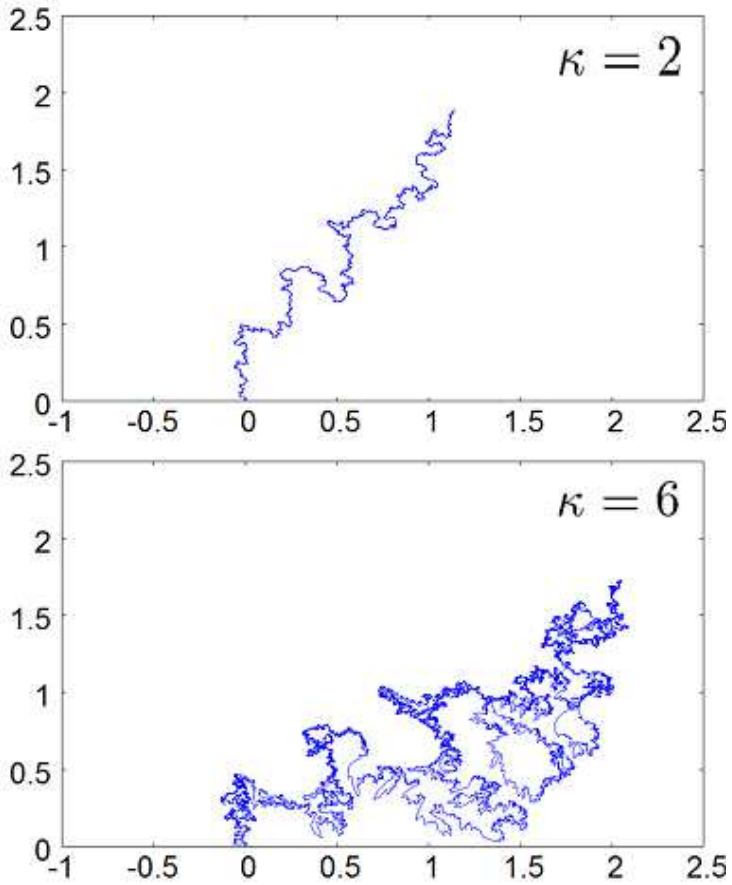


FIG. 2: Approximations of the SLE_κ curves up to time $T = 1$ expressed by the ISCT_κ paths for $\kappa = 2$ and $\kappa = 6$.

same realization of RW as a driving function, the ISCT_κ paths with large values of κ exhibit much more complicated motion on $\mathbb{H}$ than those with smaller values of κ. In Sec.IV, we report the properties of the rescaled ISCT paths $\zeta^N(0,T]$ with $T = 1$ based on large scaled computer simulations with $N \simeq 10^4 \sim 10^5$. We evaluate the fractal dimensions d^κ_{ISCT} of the $N \to \infty$ limits of $\zeta^N(0,1]$ for several values of κ, and the dependence of d^κ_{ISCT} on κ is compared with that of the fractal dimensions d^κ of the SLE curves given by (4). We also show that, for $4 < \kappa < 8$, the generalized version of Cardy's formula of SLE_κ curves [2, 21] will be applicable to the rescaled ISCT_κ paths $\zeta^N(0,T]$, if N and T are sufficiently large. Section V is devoted to give concluding remarks. Appendix A is prepared for giving recurrence relations, which will be useful to analyze the ISCT paths.

II. ISCT DRIVEN BY RW

Noting that Eq.(12) is solved for α as $\alpha = [1 \pm \sqrt{\kappa/(\kappa+16)}]/2$, we set

$$\alpha^\kappa(\sigma) = \frac{1}{2}\left[1 - \sigma\sqrt{\frac{\kappa}{\kappa+16}}\right] \tag{17}$$

for $\kappa > 0, \sigma \in \{-1, 1\}$, and define the SCT as a functional of a random variable σ by

$$\begin{aligned} F^\kappa_\sigma(z) &\equiv f_1^{\alpha^\kappa(\sigma)}(z) \\ &= \left(z + 2\sqrt{\frac{\alpha^\kappa(\sigma)}{1-\alpha^\kappa(\sigma)}}\right)^{1-\alpha^\kappa(\sigma)} \left(z - 2\sqrt{\frac{1-\alpha^\kappa(\sigma)}{\alpha^\kappa(\sigma)}}\right)^{\alpha^\kappa(\sigma)}. \end{aligned} \tag{18}$$

Given one step σ_1 of RW on $\mathbb{Z}$, we consider an SCT, $F^\kappa_{\sigma_1}(z)$, which is a conformal map from $\mathbb{H}$ to the region $\mathbb{H}$ with a straight slit. The straight slit starts from the origin and ends at the tip located at

$$\begin{aligned} \xi_1 &= F^\kappa_{\sigma_1}(\sqrt{\kappa}\sigma_1) \\ &= 2\left(\frac{1-\alpha^\kappa(\sigma_1)}{\alpha^\kappa(\sigma_1)}\right)^{1/2-\alpha^\kappa(\sigma_1)} e^{i\alpha^\kappa(\sigma_1)\pi}. \end{aligned} \tag{19}$$

Next assume that two steps of RW, (σ_1, σ_2), is given. We transform $\mathbb{H}$ by an SCT, $F^\kappa_{\sigma_2}$. The image of $\mathbb{H}$, $F^\kappa_{\sigma_2}(\mathbb{H})$, is the region $\mathbb{H}$ with the straight slit, which starts from the origin and ends at $\xi_2^{(1)} \equiv F^\kappa_{\sigma_2}(\sqrt{\kappa}\sigma_2)$. Then we consider the transformation of the region $\mathbb{H}$ with this straight slit by another SCT, $F^\kappa_{\sigma_1}$. By this SCT, a straight slit from the origin to the point ξ_1 is generated as shown by (19). The image by $F^\kappa_{\sigma_1}$ of the straight slit between the origin and $\xi_2^{(1)}$ in $\mathbb{H}$ is, however, no longer a straight line but a curvy one. It starts from ξ_1 and ends at

$$\begin{aligned} \xi_2 &= F^\kappa_{\sigma_1}(\sqrt{\kappa}\sigma_1 + \xi_2^{(1)}) \\ &= F^\kappa_{\sigma_1}(\sqrt{\kappa}\sigma_1 + F^\kappa_{\sigma_2}(\sqrt{\kappa}\sigma_2)). \end{aligned} \tag{20}$$

We have then a set of two points (ξ_1, ξ_2) in $\mathbb{H}$. Set $n \geq 1$ and now we assume that a realization of RW on $\mathbb{Z}$ up to time n is specified by the series of n steps, $\boldsymbol{\sigma}(n) = (\sigma_1, \sigma_2, \ldots, \sigma_n)$. Let

$$S^\kappa_\sigma(z) = F^\kappa_\sigma(\sqrt{\kappa}\sigma + z) \tag{21}$$

for $\kappa > 0, \sigma \in \{-1, 1\}$ and $z \in \mathbb{H}$. We perform the following iteration of SCTs,

$$\begin{aligned} \mathcal{S}^\kappa_{\boldsymbol{\sigma}(n)}(z) &= S^\kappa_{\sigma_1} \circ S^\kappa_{\sigma_2} \circ \cdots \circ S^\kappa_{\sigma_n}(z) \\ &\equiv S^\kappa_{\sigma_1}\Big(S^\kappa_{\sigma_2}(\cdots(S^\kappa_{\sigma_n}(z))\cdots)\Big). \end{aligned} \tag{22}$$

Then we have a curve consisting of a straight slit between the origin $\xi_0 = 0$ and ξ_1 and $n-1$ segments of curvy slits, which are sequentially connected at $\xi_j, 1 \le j \le n-1$, and the tip is at ξ_n. See Fig. 3. In the present paper we call $\mathcal{S}^{\kappa}_{\boldsymbol{\sigma}(n)}(z)$ the iterative Schwarz-Christoffel transformation (ISCT for short) driven by RW specified by $\boldsymbol{\sigma}(n) = (\sigma_1, \ldots, \sigma_n)$.

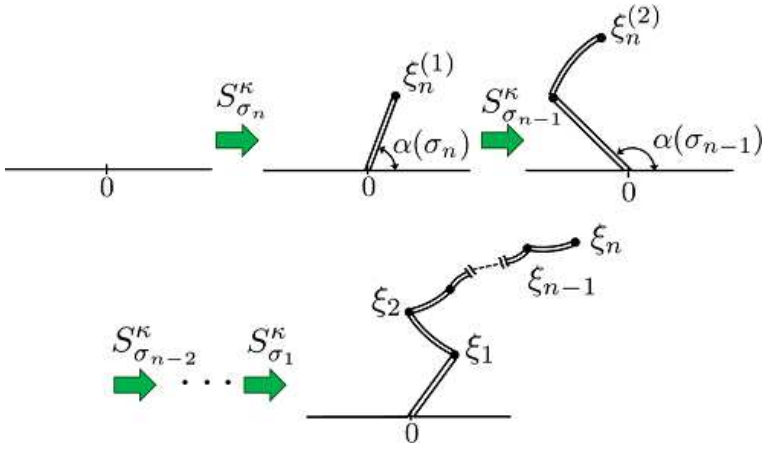


FIG. 3: Iteration of SCTs

For $n = 1, 2, 3, \ldots$, we define the points in $\mathbb{H}$ by

$$\xi_n = \mathcal{S}^{\kappa}_{\boldsymbol{\sigma}(n)}(0). \tag{23}$$

We set $\xi_0 \equiv 0$. The sequence of points $(\xi_0, \xi_1, \xi_2, \ldots, \xi_n)$ is interpolated by straight lines. We call it an ISCT path in $\mathbb{H}$ and denote it by $\Xi(0, n]$. In other words, each realization $\boldsymbol{\sigma}(n)$ of RW on $\mathbb{Z}$ is mapped to a path $\Xi(0, n]$ on $\mathbb{H}$ by the ISCT.

For a given $n \ge 1$, we introduce the following recurrence relations for a series $(\xi_n^{(0)}, \xi_n^{(1)}, \ldots, \xi_n^{(n)})$,

$$\xi_n^{(k+1)} = S^{\kappa}_{\sigma_{n-k}}(\xi_n^{(k)}), \quad k = 0, 1, 2, \ldots, n-1 \tag{24}$$

with $\xi_n^{(0)} = 0$. Since $\sigma_j, j = 1, 2, 3, \ldots, n$ are i.i.d., the recurrence formula (24) is useful to calculate the position ξ_n, which is given by $\xi_n^{(n)}$. Moreover, if we introduce a parameter $\theta \in (0, \pi/2)$ with the relation

$$\cos\theta = \sqrt{\frac{\kappa}{\kappa + 16}}, \tag{25}$$

(17) is written as

$$\begin{aligned} \alpha^{\kappa}(\sigma) &= \frac{1}{2}(1 - \sigma\cos\theta) \\ &= \begin{cases} \sin^2(\theta/2), & \sigma = 1 \\ \cos^2(\theta/2), & \sigma = -1, \end{cases} \end{aligned} \tag{26}$$

and (19) is given by

$$\begin{aligned}\xi_1 &= S^{\kappa}_{\sigma_1}(0) \\ &= \begin{cases} 2(\cot(\theta/2))^{\cos 2\theta} e^{i\pi \sin^2(\theta/2)}, & \sigma_1 = 1 \\ 2(\cot(\theta/2))^{\cos 2\theta} e^{i\pi \cos^2(\theta/2)}, & \sigma_1 = -1. \end{cases}\end{aligned} \tag{27}$$

Note that $\xi_1(\sigma = -1) = -(\xi_1(\sigma = 1))^*$, where * indicates complex conjugate. The recurrence relation (24) is then written as

$$\xi_n^{(k+1)} = \left(\xi_n^{(k)} + \sigma_{n-k} \cot\frac{\theta}{2}\right)^{\cos^2(\theta/2)} \left(\xi_n^{(k)} - \sigma_{n-k} \tan\frac{\theta}{2}\right)^{\sin^2(\theta/2)}, \quad k = 0, 1, 2, \ldots, n-1 \tag{28}$$

for $\sigma_{n-k} = \pm 1$ with $\xi_n^{(0)} = 0$. The expressions for the relations between two real components of complex variable $\xi_n^{(k+1)}$ and those of $\xi_n^{(k)}$ are given in Appendix A.

III. NETWORKS ON $\mathbb{H}$ GENERATED BY RW PATHS

For a fixed time period $n > 0$, consider a collection of all realization of steps of RW on $\mathbb{Z}$,

$$\mathcal{F}(n) = \Big\{ \boldsymbol{\sigma}(n) = (\sigma_1, \sigma_2, \ldots, \sigma_n) : \sigma_j \in \{-1, 1\}, 1 \le j \le n \Big\}. \tag{29}$$

The total number of realizations of RWs is $|\mathcal{F}(n)| = 2^n$. We note that each realization of RW up to time $n > 0$ is represented by a directed path on a squared lattice in a triangular region in the spatio-temporal plane,

$$\Lambda_n = \Big\{ (j, k) \in \mathbb{Z} \times \{0, 1, 2, \ldots\} : 0 \le k \le n, -k \le j \le k, j + k = \text{even} \Big\}. \tag{30}$$

Here any edge connecting nearest neighbor vertices in Λ_n is assumed to be directed in the positive direction of the time axis; $(j, k) \to (j \pm 1, k + 1)$, and each path is a sequence of edges all in the positive direction, starting from $(0, 0)$ to (j, n) with $-n \le j \le n$. Figure 4 shows Λ_4 and an example of a realization of RW with $\boldsymbol{\sigma}(4) = (1, 1, -1, 1)$.

By collecting all ISCT paths up to time n, $\Xi(0, n]$, we have a network on $\mathbb{H}$,

$$\mathcal{N}_n^{\kappa} = \Big\{ \Xi(0, n] : \Xi_j = S^{\kappa}_{\boldsymbol{\sigma}(j)}(0), 1 \le j \le n, \boldsymbol{\sigma}(n) \in \mathcal{F}(n) \Big\}. \tag{31}$$

Figure 5 shows $\mathcal{N}_n^{\kappa}$ for $\kappa = 2, 4, 6$ and 8 for $n = 4$. As the parameter κ increases, the network becomes spreading wider in $\mathbb{H}$. There the ISCT path corresponding to the realization of RW

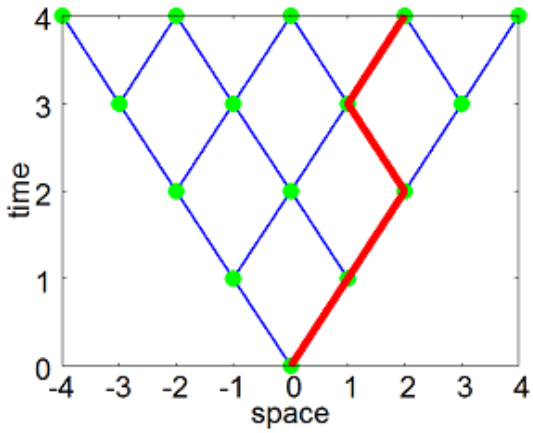


FIG. 4: Lattice Λ_4 and one realization of RW with $\boldsymbol{\sigma}(4) = (1, 1, -1, 1)$.

$\boldsymbol{\sigma}(4) = (1, 1, -1, 1)$ shown in Fig. 4 is indicated by a bold line for each value of κ. In Fig. 6, we compare the ISCT paths with (b) $\kappa = 2$ and (c) $\kappa = 8$ both obtained from the same realization (a) of RW with $n = 20$ steps, where the networks up to $n = 10$, $\mathcal{N}_{10}^{\kappa}$, are also shown in the background for each κ. We can see that the ISCT path with $\kappa = 8$ is much more complicated than the path with $\kappa = 2$. As shown by Fig.5 and Fig.6, the network $\mathcal{N}_n^{\kappa}$ is bounded by the rightmost path $\Xi^{\max}(0, n]$ generated by $\boldsymbol{\sigma}_{\max}(n) = (1, 1, \ldots, 1)$ and the leftmost path $\Xi^{\min}(0, n]$ generated by $\boldsymbol{\sigma}_{\min}(n) = (-1, -1, \ldots, -1)$. The height of $\Xi_n^{\max}$ and $\Xi_n^{\min}$, $H_n^{\kappa} = \mathrm{Im}\,\Xi_n^{\max} = \mathrm{Im}\,\Xi_n^{\min}$, is observed to converge to a positive constant H_{∞}^{κ} in $n \to \infty$. The numerical values are given by $H_{\infty}^{\kappa} = 0.014 (\kappa = 1)$, 0.010 $(\kappa = 2)$, 0.0084 $(\kappa = 3)$, 0.0074 $(\kappa = 4)$, 0.0067 $(\kappa = 5)$, 0.0062 $(\kappa = 6)$, 0.0058 $(\kappa = 7)$, and 0.0055 $(\kappa = 8)$.

IV. NUMERICAL ANALYSIS OF CURVES GENERATED BY ISCT

For a given number of steps $n = NT$ of RW, we have defined the rescaled ISCT path $\zeta^N(0, T]$ by Eq.(16). In particular, $\zeta(0, 1]$ is obtained by interpolating the series of points $\{\xi_j/\sqrt{N}\}_{j=0}^{N}$ by straight lines. We have studied statistical properties of the rescaled ISCT paths based on the numerical data of large scaled computer simulations.

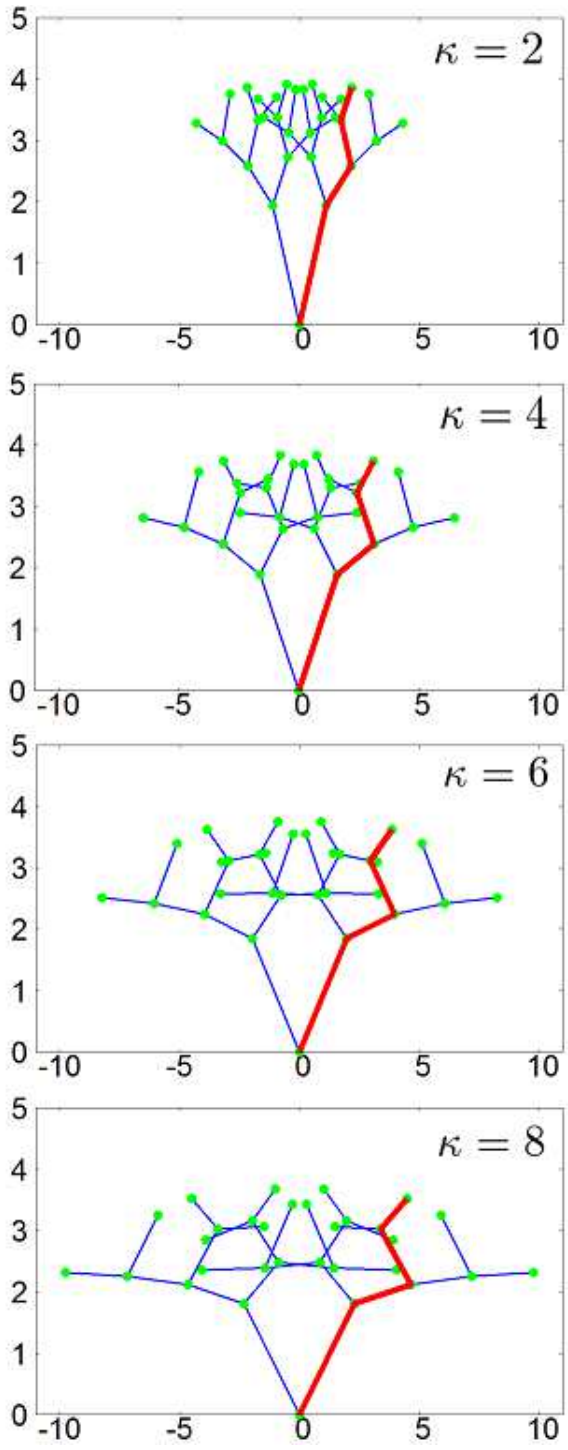


FIG. 5: Networks $\mathcal{N}_n^\kappa$ on $\mathbb{H}$ for $n = 4$ with $\kappa = 2, 4, 6, 8$. The ISCT paths corresponding to the same realization of RW $\boldsymbol{\sigma}(4) = (1, 1, -1, 1)$ are indicated by bold lines.

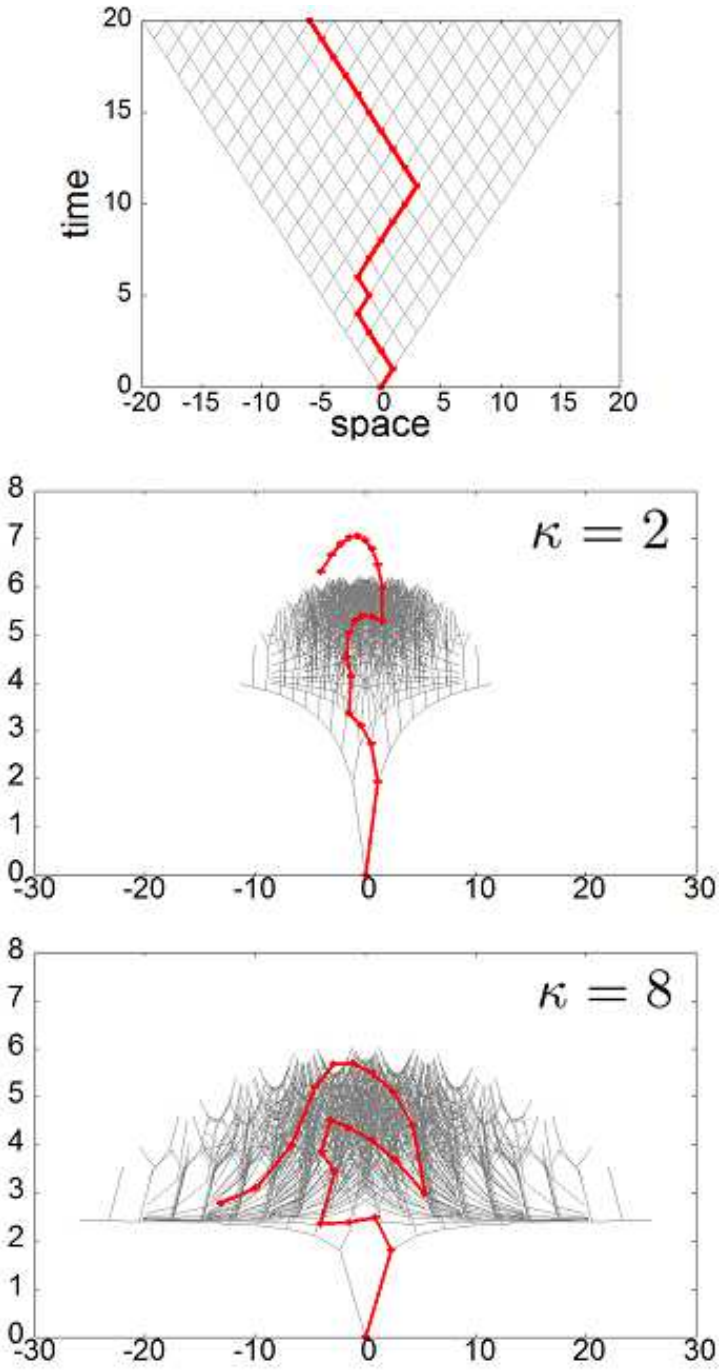


FIG. 6: (a) A realization of RW with time step $n = 20$. (b) The ISCT path for $\kappa = 2$ generated from the RW shown in (a) with the network $\mathcal{N}_{10}^{2}$. (c) The ISCT path for $\kappa = 8$ generated from the same RW shown in (a) with the network $\mathcal{N}_{10}^{8}$.

A. Fractal Dimensions

Figure 7 shows a log-log plot of the box counting of segments of $\zeta^N(0,1]$ with respect to the box sizes for $\kappa = 4$ with $N = 5 \times 10^4$. As shown by this figure, the data for any κ can be fitted by a straight line very well and we can evaluate the approximate values of fractal dimensions for finite N.

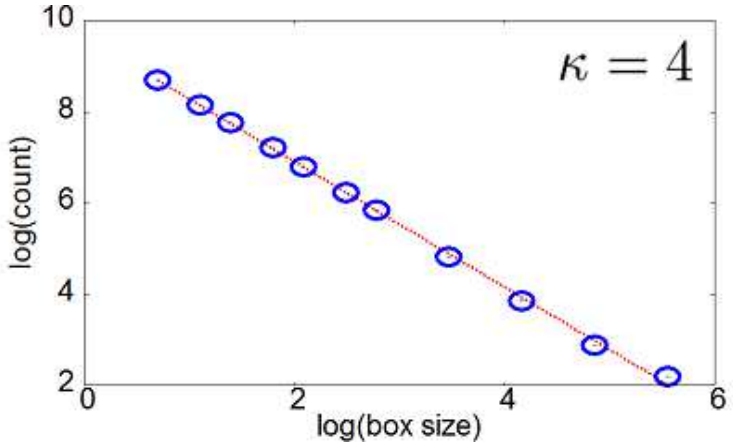


FIG. 7: Log-log plot of the box-counting data for the restricted ISCT paths for $\kappa = 4$.

The evaluated values up to at most $N = 3 \times 10^5$ are then plotted versus $1/N$ in Fig.8. For each evaluation we prepared $M = 20$ samples, and the ranges of scattering of results are shown by error bars in the figure. There $N \to \infty$ limits are extrapolated by three-parameter fittings ; $d = a_0 + a_1/N + a_2/N^2$. The obtained values a_0 by the extrapolation are denoted by $d^\kappa_{\rm ISCT}$.

Figure 9 shows dependence of $d^\kappa_{\rm ISCT}$ on κ. The Hausdorff dimensions of the SLE$_\kappa$ curves given by (4) are also shown by a dotted line. Systematic deviation is found between d^κ for the SLE curves and $d^\kappa_{\rm ISCT}$ numerically evaluated for the rescaled ISCT paths. We observe in Fig.8 that the approximate value of fractal dimension for finite N is increasing as N is increasing, and the ratio of increment becomes larger as κ approaches the value 8. So we expect that the deviation will be systematically reduced, if we can perform numerical simulation for larger N's and make appropriate extrapolation to the $N \to \infty$ limit.

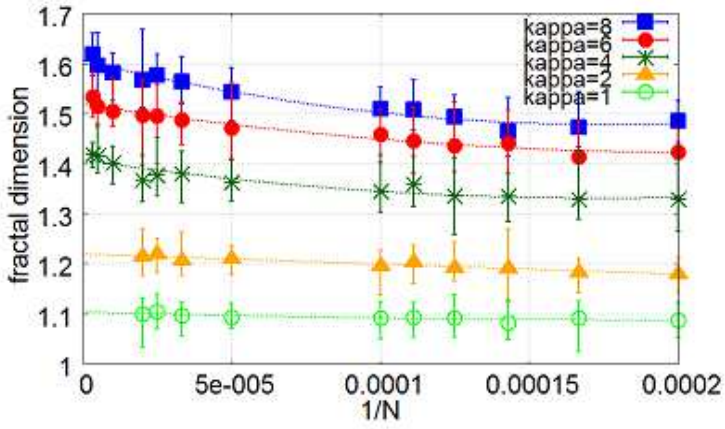


FIG. 8: Extrapolation of fractal dimensions in the $N \to \infty$ limit.

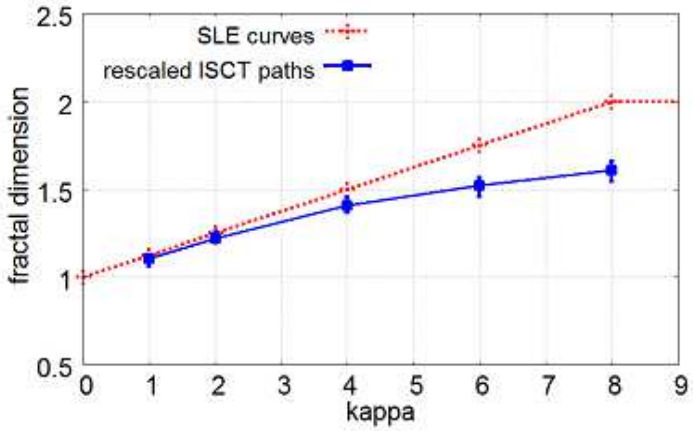


FIG. 9: Dependence of the fractal dimensions $d^{\kappa}_{\rm ISCT}$ of rescaled ISCT paths is shown. The Hausdorff dimensions of the SLE$_\kappa$ curves given by Eq.(4) are also plotted by a dotted line.

B. Generalized Cardy's Formula

Here we first consider the SLE curve $\gamma(0,\infty) = \{\gamma_t : 0 < t < \infty\}$ in the case

$$4 < \kappa < 8. \tag{32}$$

In this case, γ_t starting from the origin will hit the real axis $\mathbb{R}$ infinitely many times [2, 3]. For $x > 0$ we can define

$$t_*(x) \;=\; \text{the first time, when } \gamma_t \text{ hits a point in } [x,\infty) \text{ on } \mathbb{R}. \tag{33}$$

Then, $\gamma_{t_*(x)}$ is the leftmost point in the interval $[x, \infty)$, at which γ_t hits $\mathbb{R}$. Note that, if $\kappa \leq 4$, $t_*(x) = \infty$, and if $\kappa \geq 8$, $\gamma_{t_*(x)} = x$, with probability one. For (32), $\gamma_{t_*(x)}$ has a nontrivial distribution. For each $\varepsilon > 0$, we observe whether $\xi_{t_*(x)} < x + \varepsilon$ or $\xi_{t_*(x)} \geq x + \varepsilon$. Figure 10 illustrates the former case. For the SLE_κ curves with (32), the following formula is established. (See Proposition 6.34 in [2].)

$$\begin{aligned} \mathrm{P}(\gamma_{t_*(x)} < x + \varepsilon) &= \frac{\Gamma(4/\kappa)}{\Gamma(8/\kappa - 1)\Gamma(1 - 4/\kappa)} \int_0^{\varepsilon/(x+\varepsilon)} u^{8/\kappa - 2}(1-u)^{-4/\kappa} du \\ &= \frac{\Gamma(4/\kappa)}{\Gamma(8/\kappa)\Gamma(1 - 4/\kappa)} \left(\frac{\varepsilon}{x+\varepsilon}\right)^{8/\kappa - 1} F\left(\frac{4}{\kappa}, \frac{8}{\kappa} - 1, \frac{8}{\kappa}; \frac{\varepsilon}{x+\varepsilon}\right), \end{aligned} \tag{34}$$

where $\Gamma(z)$ is the gamma function and $F(\alpha, \beta, \gamma; z)$ is Gauss's hypergeometric function. This formula can be regarded as a generalization of Cardy's formula, since the original formula corresponding to (34) with $\kappa = 6$ was derived by Cardy [21] for the "percolation exploration process" in the critical percolation model, and then the continuum limit of that process was proved to be described by the SLE curve with $\kappa = 6$ [15, 16]. For $0 < \varepsilon \ll 1$, the above formula gives a power law

$$\mathrm{P}(\gamma_{t_*(x)} < x + \varepsilon) \simeq \left(\frac{\varepsilon}{x}\right)^{\delta(\kappa)} \tag{35}$$

with the exponent

$$\delta(\kappa) = \frac{8 - \kappa}{\kappa} \tag{36}$$

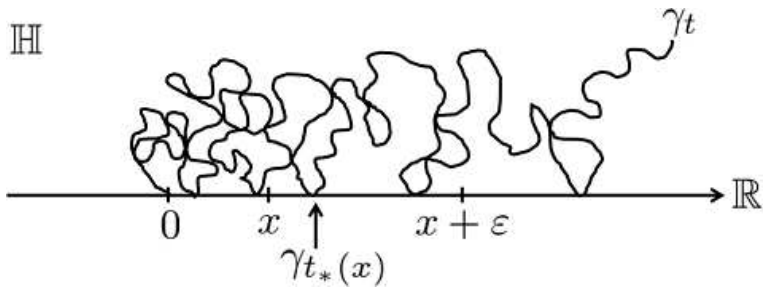


FIG. 10: Illustration of the point $\gamma_{t_*(x)}$ on the real axis $\mathbb{R}$ for an SLE_κ curve with $4 < \kappa < 8$.

Now we consider the ISCT paths. For integers N and T with $N \gg 1$, prepare a realization of RW represented by $\boldsymbol{\sigma}(NT) = (\sigma_1, \sigma_2, \ldots, \sigma_{NT})$. For each $n = 1, 2, \ldots, NT$, by using the data $(\sigma_1, \sigma_2, \ldots, \sigma_n)$, we calculate the position ξ_n in $\mathbb{H}$ following the recurrence formula (24). As noted at the end of Sec.III, $\mathrm{Im}\, \xi_n > 0$ for any $n \geq 1$. So we set a small value $h > 0$ and look for the event

$$\mathcal{E}_{h,x}^N(n) = \left\{ \frac{\mathrm{Im}\, \xi_n}{\sqrt{N}} < h \quad \text{and} \quad \frac{\mathrm{Re}\, \xi_n}{\sqrt{N}} \geq x \right\}. \tag{37}$$

We define

$$n_h(x) = \min\Big\{n : 1 \le n \le NT,\ \mathcal{E}^N_{h,x}(n) \text{ occurs}\Big\}. \tag{38}$$

If $n_h(x) \le NT$, we define $t_h(x) = n_h(x)/N$ and calculate the value $\mathrm{Re}\,\zeta^N_{t_h(x)} = \mathrm{Re}\,\Xi^N_{Nt_h(x)}/\sqrt{N} = \mathrm{Re}\,\xi^N_{n_h(x)}/\sqrt{N}$. If $n_h(x) > NT$, that is, the event (37) does not occur for the given $\boldsymbol{\sigma}(NT)$, then $t_h(x) > T$. The probability distribution function for the rescaled ISCT paths, which corresponds to $P(\gamma_{t_*(x)} < x + \varepsilon)$, may be given by

$$\lim_{h\to 0}\lim_{T\to\infty}\lim_{N\to\infty} \mathrm{P}\Big(\mathrm{Re}\,\zeta^N_{t_h(x)} < x + \varepsilon,\ t_h(x) \le T\Big) \equiv \mathrm{P}(\zeta_{t_*(x)} < x + \varepsilon), \tag{39}$$

where $\zeta(0,\infty) = \lim_{T\to\infty}\lim_{N\to\infty}\zeta^N(0,T]$.

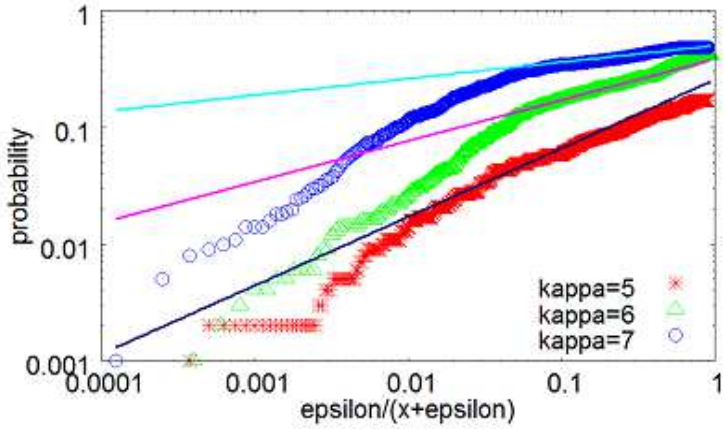


FIG. 11: Log-log plots of the numerical evaluations of the probability $\mathrm{P}(\mathrm{Re}\,\zeta^N_{t_h(x)} < x+\varepsilon,\ t_h(x) < 1)$ versus $\varepsilon/(x+\varepsilon)$ for the rescaled ISCT paths.

In numerical calculations, we have set $N = 10^4$ and $T = 1$ and prepared $M = 1000$ realizations of RW, which are randomly generated. Since $T = 1$, we are allowed to consider only small values of x and ε. The threshold value h is wanted to be small, but for finiteness of N, it should be positive. In Fig.11, we show log-log plots of the numerical evaluations of $\mathrm{P}(\mathrm{Re}\,\zeta^N_{t_h(x)} < x + \varepsilon,\ t_h(x) \le 1)$ for $\kappa = 5$ with $x = 0.8, h = 0.1$, $\kappa = 6$ with $x = 0.5, h = 0.1$, and $\kappa = 7$ with $x = 0.8, h = 0.2$. For finiteness of N and smallness of the number of samples M, data scatter for small ε. We find, however, power-law behaviors in the intermediate regions of ε;

$$\mathrm{P}(\zeta_{t_*(x)} < x + \varepsilon) \simeq \varepsilon^{\delta}. \tag{40}$$

By linear fitting as shown in Fig.11, we have evaluated the values of exponent δ. The results are plotted in Fig.12, where Eq.(36) derived from the generalized Cardy's formula is also

shown by a curve. The good agreement implies that in the proper limit (39) will also follow the generalized Cardy's formula in the parameter region (32).

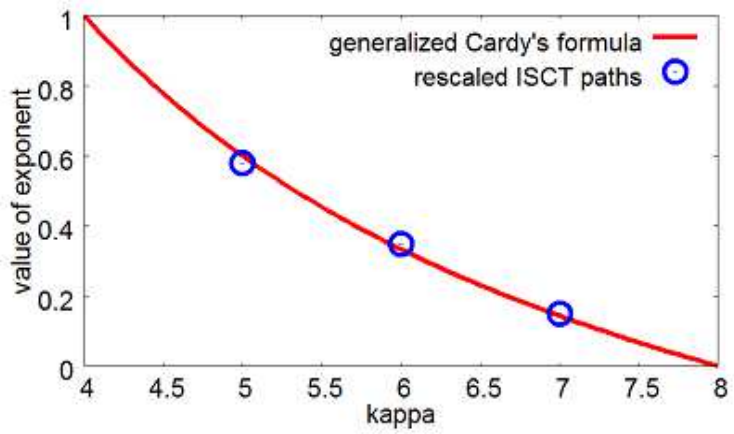


FIG. 12: Numerical evaluations of the exponent δ in the power law (40) for $\kappa = 5, 6$, and 7. The curve shows Eq.(36) of the generalized Cardy's formula.

V. CONCLUDING REMARKS

In the present paper, we have proposed an algorithm, which generates a random discrete path $\Xi(0, NT]$ on the upper half complex-plane $\mathbb{H}$ as a functional of a path of random walk $W(0, NT]$ on the real axis $\mathbb{R}$ for integers N and T. The system has one parameter $\kappa > 0$ and we call the path an ISCT_κ path. We have studied the rescaled ISCT_κ path defined by $\zeta^N(0, T] = \Xi(0, NT]/\sqrt{N}$ for large N by computer simulations. The numerical analysis of the distributions of $\zeta^N(0, T]$ supports our expectation that the limits of the rescaled ISCT_κ paths $\zeta(0, \infty) = \lim_{T\to\infty} \lim_{N\to\infty} \zeta^N(0, T]$ will have the same statistical properties as the SLE_κ curves have.

The rescaled ISCT_κ paths $\zeta^N(0, T]$ can be regarded as discrete approximations of the SLE_κ curves. In this sense, the present study could be included by the previous numerical work [17, 18]. In this paper, however, we have emphasized on our interest in the ISCT itself as a simple algorithm to generate complicated discrete dynamics of a point on $\mathbb{H}$. Dependence on the parameter κ of complexity of the SLE curves is demonstrated by dependence of complexity of the network $\mathcal{N}_n^\kappa$ of the ISCT paths on the angle $\alpha\pi$ of the slit generated by a single SCT.

We have learned that stochastic analysis is necessary and useful to study statistics and stochastics of the SLE_κ curves [2, 3]. Although we have reported only numerical study in this paper, we hope that the combinatorics and statistical mechanics methods developed for solvable models on lattices will be useful to analyze statistics and stochastics of the ISCT_κ paths on $\mathbb{H}$, since they are functionals of simple random walks in one dimension.

Acknowledgments

The present authors would like to thank M. Matsushita and N. Kobayashi for useful discussion on application of the fractal analysis to the present work. This work was partially supported by the Grant-in-Aid for Scientific Research (C) (No.21540397) of Japan Society for the Promotion of Science.

Appendix A: Recurrence Relations

Let $\xi_n^{(k)} = 2re^{i\phi}, r > 0, 0 < \phi < \pi$ for $k < n$. Then (28) gives

$$\xi_n^{(k+1)} = 2R_{\sigma_{n-k}} \exp(i\Phi_{\sigma_{n-k}}), \quad \sigma_{n-k} = \pm 1 \tag{A1}$$

with

$$\begin{aligned} R_\sigma &= 2\left(r^2 + 2\sigma r\cos\phi\cot\frac{\theta}{2} + \cot^2\frac{\theta}{2}\right)^{(\cos^2(\theta/2))/2} \\ &\quad \times \left(r^2 - 2\sigma r\cos\phi\tan\frac{\theta}{2} + \tan^2\frac{\theta}{2}\right)^{(\sin^2(\theta/2))/2}, \end{aligned} \tag{A2}$$

$$\begin{aligned} \Phi_\sigma &= \arccos\left(\frac{r\cos\phi + \sigma\cot(\theta/2)}{\sqrt{r^2 + 2\sigma r\cos\phi\cot(\theta/2) + \cot^2(\theta/2)}}\right)\cos^2\frac{\theta}{2} \\ &\quad + \arccos\left(\frac{r\cos\phi - \sigma\tan(\theta/2)}{\sqrt{r^2 - 2\sigma r\cos\phi\tan(\theta/2) + \tan^2(\theta/2)}}\right)\sin^2\frac{\theta}{2} \end{aligned} \tag{A3}$$

When we set $\xi_n^{(k)} = 2(x + iy), x \in \mathbb{R}, y > 0, k < n$, the above gives

$$\xi_n^{(k+1)} = 2(X_{\sigma_{n-k}} + iY_{\sigma_{n-k}}), \quad \sigma_{n-k} = \pm 1 \tag{A4}$$

with

$$X_\sigma = \left(x^2+y^2+2\sigma x\cot\frac{\theta}{2}+\cot^2\frac{\theta}{2}\right)^{(\cos^2(\theta/2))/2}\left(x^2+y^2-2\sigma x\tan\frac{\theta}{2}+\tan^2\frac{\theta}{2}\right)^{(\sin^2(\theta/2))/2}$$
$$\times\cos\left[\arccos\left(\frac{x+\sigma\cot(\theta/2)}{\sqrt{x^2+y^2+2\sigma x\cot(\theta/2)+\cot^2(\theta/2)}}\right)\cos^2\frac{\theta}{2}\right.$$
$$\left.+\arccos\left(\frac{x-\sigma\tan(\theta/2)}{\sqrt{x^2+y^2-2\sigma x\tan(\theta/2)+\tan^2(\theta/2)}}\right)\sin^2\frac{\theta}{2}\right], \tag{A5}$$

$$Y_\sigma = \left(x^2+y^2+2\sigma x\cot\frac{\theta}{2}+\cot^2\frac{\theta}{2}\right)^{(\cos^2(\theta/2))/2}\left(x^2+y^2-2\sigma x\tan\frac{\theta}{2}+\tan^2\frac{\theta}{2}\right)^{(\sin^2(\theta/2))/2}$$
$$\times\sin\left[\arccos\left(\frac{x+\sigma\cot(\theta/2)}{\sqrt{x^2+y^2+2\sigma x\cot(\theta/2)+\cot^2(\theta/2)}}\right)\cos^2\frac{\theta}{2}\right.$$
$$\left.+\arccos\left(\frac{x-\sigma\tan(\theta/2)}{\sqrt{x^2+y^2-2\sigma x\tan(\theta/2)+\tan^2(\theta/2)}}\right)\sin^2\frac{\theta}{2}\right]. \tag{A6}$$

---

[1] O. Schramm, Israel J. Math. **118**, 221 (2000).

[2] G. F. Lawler, *Conformally Invariant Processes in the Plane*, (American Mathematical Society, 2005).

[3] G. Lawler, e-print arXiv: 0712.3256 [math.PR].

[4] W. Kager and B. Nienhuis, J. Stat. Phys. **115**, 1149 (2004).

[5] J. Cardy : Ann. Phys. **318**, 81 (2005).

[6] M. Bauer and D. Bernard, Phys. Rep. **432**, 115 (2006).

[7] C. Pommerenke, *Univalent Functions*, (Vandenhoeck & Ruprecht, Götingen, 1975).

[8] J. Cardy, e-print arXiv: math-ph/0103018.

[9] M. Bauer and D. Bernard, Phys. Lett. **B 557**, 309 (2003).

[10] R. Friedrich and W. Werner, Commun. Math. Phys. **243**, 105 (2003).

[11] Loewner considered conformal maps from a unit disk $\mathbb{D}=\{z\in\mathbb{C}:|z|<1\}$ to one-slit domains $\mathbb{D}\setminus\gamma$ with a slit starting from a point on the circle $\partial\mathbb{D}=\{z\in\mathbb{C}:|z|=1\}$, and used a different equation from (2). In the present paper, we consider a modified version suitable for $\mathbb{H}$ and discuss the *chordal* Loewner equation (LE) rather than the original *radial* LE.

[12] Usually the time evolution of the inverse map $g_t=f_t^{-1}$ given by $\partial g_t/\partial t=2/(g_t-\sqrt{\kappa}B_t)$ is called the SLE. Since f_t is one-to-one, $\partial f_t/\partial z\neq 0$, f_t can determine g_t completely.

[13] V. Beffara, Ann. Probab. **36**, 1421 (2008).

[14] G. Lawler, in *Fractal Geometry and Stochastics IV, (Progress in Probability, Vol. 61)*, edited by C. Babdt, P. Mörters, M. Zähle, (Birkhäuser, 2009), pp. 73-107.

[15] S. Smirnov, C. R. Acad. Sci. Paris Sér. I Math. **333**, 239 (2001).

[16] V. Beffara, in *Universality and Renormalization : From Stochastic Evolution to Renormalization of Quantum Fields, (Fields Institute Communications, Vol.50)*, edited by I. Binder and D. Kreimer, (American Mathematical Society, 2007), pp. 39-45.

[17] T. Kennedy, J. Stat. Phys. **128**, 1125 (2007).

[18] T. Kennedy, J. Stat. Phys. **137**, 839 (2009).

[19] Y. Kondo, N. Mitarai, and H. Nakanishi, Phys. Rev. E **80**, 050102(R) (2009).

[20] M. J. Ablowitz and A. S. Fokas, *Complex Variables, Introduction and Applications*, 2nd ed., (Cambridge University Press, Cambridge, England, 2003).

[21] J. Cardy, J. Phys. A **25**, L201 (1992).